

# Localization of a Silent Target Node in Magnetic Induction based Wireless Underground Sensor Networks

S. Kisseleff <sup>▲</sup>, X. Chen <sup>▲</sup>, I. F. Akyildiz <sup>★</sup>, and W. Gerstacker <sup>▲</sup>

<sup>▲</sup> Institute for Digital Communications, Friedrich-Alexander University (FAU), Erlangen-Nürnberg, Germany  
 steven.kisseleff@fau.de, xiaoyang.chen@studium.fau.de, wolfgang.gerstacker@fau.de

<sup>★</sup> Broadband Wireless Networking Lab, Georgia Institute of Technology, USA, ian@ece.gatech.edu

**Abstract**—Wireless underground sensor networks (WUSNs) based on magnetic induction (MI) have been recently proposed as a promising candidate for underground networking. The benefit of the MI-WUSNs compared to other solutions (e.g. so-called Through-The-Earth communication) is related to the substantially lower path loss and lower vulnerability to the changes of the soil properties. In the past, some efforts have been made to characterize the signal transmission in MI-WUSNs. Those investigations, however, refer mostly to the information transmission. One of the target applications of the WUSNs is the object localization in the underground medium, which remains an open issue due to the complicated characteristics of the MI channels corrupted by the influence of soil. In this work, we propose a machine learning based solution for localization. In addition, a novel passive localization technique is introduced, which requires no signal from the target node and thus proves useful for rescue operations, where the battery of the node to be localized is either empty or damaged.

## I. INTRODUCTION

Typical applications of Wireless Underground Sensor Networks (WUSNs) include earthquake prediction, communication in mines/tunnels, monitoring of the underground medium for agricultural purposes, etc. [1]. Due to the harsh propagation conditions in the soil medium, in particular a high path loss and time varying changes of soil properties [2], the use of traditional wireless signal propagation techniques based on electromagnetic (EM) waves is mostly infeasible.

In order to cope with these problems, magnetic induction (MI) based WUSNs have been introduced in [3], where induction coils have been employed as antennas. This technique has been shown to be less vulnerable to the losses in a conductive medium, such that the transmission range and coverage of a sensor network can be significantly improved by using MI based transceivers. Most of the works in this area aimed at solving various problems of MI-WUSNs with respect to information transmission. For example, some efforts have been made to characterize the transmission channel [3], the signal quality [4], and the network throughput of MI-WUSNs [5], [6]. In these works, the influence of different environmental and system parameters on the signal propagation has been studied

for various conditions. Several groups have also conducted experiments in order to verify the most common assumptions for the utilized system models, cf. [7], [8], [9].

In this work, we study localization techniques for MI-WUSNs. MI based localization has been investigated in some previous works, e.g. [10], [11], and [12]. However, these works do not explicitly consider the localization in the underground environment, which has substantially different characteristics and challenges compared with the over-the-air transmission, as known from [2]. Hence, the methods proposed in these works may not be applicable to MI-WUSNs. The main purposes of localization in the underground medium are tracking of animal wildlife (cf. [13], [14]) and positioning of people and robots in mines (cf. [15], [16]). In [13], MI transceivers are employed in order to localize little badgers and rabbits in their natural habitat. However, the localization and tracking is not based on instantaneous observations, but on a long-term data gathering, in contrast to our work. A more advanced scheme is proposed in [14], where large coils deployed above ground are utilized. Although a good localization accuracy has been demonstrated, the presented method is only applicable to the localization in very small sized areas, as a consequence of a very high deployment effort. More relevant studies for our work are related to the localization of humans trapped in mines and provided in [15] and [16] which, however, utilize different transmission techniques (ZigBee, RFID). As argued in [17], the use of MI transceivers is justified in mines because of possible disasters and cave-ins. Hence, wearable magnetic devices attached to the bodies of mine workers can be used to localize trapped miners in case of possible disasters. For this, we assume as a worst-case scenario that the whole mine area collapses and the medium becomes homogeneous.

Typically, the localization systems based on WSNs require a signal to be transmitted by the target node for the calculation of relative distances/angles and the most likely target position [18]. This implies that the target node has to transmit continuously and that the mine worker would be permanently exposed to a magnetic field. Furthermore, the battery of the wearable target node can be empty or damaged due to a sudden disaster. In order to be able to localize such silent nodes, we assume that the transmit signal from the target node is permanently

This work was supported by the German Research Foundation (Deutsche Forschungsgemeinschaft, DFG) under Grant No. GE 861/4-2.

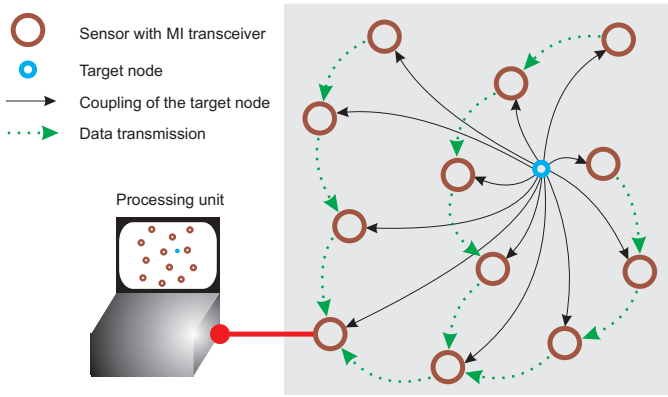


Fig. 1. Example of MI-WUSN in localization mode and a single target node. The sink node (lower left corner) collects the data from other nodes and sends it to a processing unit.

absent and design a localization approach for such a scenario. Hence, the localization is only based on signals transmitted by other sensor nodes. For this, the coupling between coils can be exploited, since the presence of the target node may significantly change the local strength of the magnetic field. The change of the field strength can be extracted and analyzed e.g. for channel estimation [19] and disaster detection [17]. We adopt this strategy for the localization of a single target node. Due to a complicated path loss function, the traditional trilateration approach may not always provide a sufficient accuracy, such that a machine learning based localization is advocated for MI-WUSNs. Furthermore, a hybrid localization method based on a combination of machine learning and trilateration is proposed, which additionally reduces the risk of outliers.

This paper is organized as follows. Section II describes the underlying system model and the signal acquisition for the localization of a single silent target node in MI-WUSNs. The signal processing for the localization via trilateration and machine learning is addressed in Section III. In Section IV, numerical results are presented and Section V concludes the paper.

## II. SYSTEM MODEL

In this work, we assume a uniform distribution of  $N_{sn}$  sensor nodes in the underground medium. The position of these nodes is random. Furthermore, all sensors have identical structure and system parameters, in order to simplify the system design and reduce the realization costs. In addition, we assume a single target node that needs to be localized by the sensor network, see Fig. 1. This target node is essentially a wearable device, which implies that it should be small and lightweight compared to the sensor nodes deployed stationary in the soil. Hence, the system parameters of the target node differ from that of the sensor nodes. In the following, we add a subscript  $S$  to the system parameters of the sensors and a subscript  $T$  to the system parameters of the target node, respectively. Also, we use the subscript  $S-S$  for the parameters of the coupling between two sensor nodes and

$S-T$  for the parameters of the coupling between a sensor node and the target node.

Since the focus of this work lies on the detection of a silent target, we exploit the magnetic coupling between all devices in the considered MI network (including the target node itself) and propose a localization approach using the signals transmitted and received at the respective sensor nodes. A similar approach has been proposed in [19] for channel estimation. At first, the signal received at the load impedance of the transmitting device is sampled. Then, a mean value among the samples within one time slot is obtained, which represents the expectation value of the detected signal magnitude<sup>1</sup> and can be delivered to the sink node via multihop relaying [5]. The sink node is assumed to be connected to a central processing unit, which collects the information from all nodes (and all time slots) and performs a processing for the localization purpose using the methods described in Section III.

Each node circuit includes a coil with inductivity  $L_S$  (or  $L_T$ ), a capacitor with capacitance  $C_S$  (or  $C_T$ ), a parasitic copper resistance  $R_S$  (or  $R_T$ ), and a load resistor  $R_{L,S}$  (or  $R_{L,T}$ ). The capacitor is designed to make the circuits resonant at center frequency  $f_0 = \frac{1}{2\pi\sqrt{L_S C_S}} = \frac{1}{2\pi\sqrt{L_T C_T}}$ . Each sensor node  $k$  is connected to a voltage source that operates at resonance frequency and transmits a sine wave given by  $u_{in,S,k}(t) = \text{Re}\{\hat{u}_{in,S,k} \cdot e^{j2\pi f_0 t}\}$  with a constant real-valued amplitude<sup>2</sup>  $\hat{u}_{in,S,k}$ . Assuming a transmit power<sup>3</sup>  $P_k \approx \frac{\hat{u}_{in,S,k}^2}{2(R_S + R_{L,S})}$ ,  $\forall k$  according to [5], the magnitude of the corresponding transmit voltage  $\hat{u}_{in,S,k} \approx \sqrt{2P_k(R_S + R_{L,S})}$ ,  $\forall k$  is obtained. Since the transmit power of all sensor nodes can be assumed identical, the magnitudes of all transmit voltages are equal, i.e.,  $\hat{u}_{in,S,k} = \hat{u}_{in,S,1}$ ,  $\forall k$ . The signal  $u_{out,S,l}(t)$  received at the load resistor of the sensor node  $l$  is transformed to equivalent complex baseband, such that only the corresponding amplitude  $\hat{u}_{out,S,l}$  is further processed. The copper resistance of the coil wires can be determined via

$$R_S = \rho \cdot \frac{2a_S N_S}{r_w^2}, \quad R_T = \rho \cdot \frac{2a_T N_T}{r_w^2} \quad (1)$$

for the sensors and the target, respectively. Here,  $N_{S/T}$  denotes the number of coil windings,  $a_{S/T}$  is the radius of the coil, and  $\rho \approx 1.678 \cdot 10^{-2} \Omega \text{mm}^2/\text{m}$  is the copper resistivity. For our investigations, the optimal value for the load resistors of the magnetic transceivers according to [20] is selected, such that  $R_{L,S} = R_S$  and  $R_{L,T} = R_T$  holds. We model the coils as magnetic dipoles and correspondingly obtain for the mutual inductance for the  $S-S$  case and  $S-T$  case, respectively,

$$M_{S-S,k,l} = \mu\pi N_S^2 \frac{a_S^4 G_{S-S,k,l}}{4r_{S-S,k,l}^3} J_{S-S,k,l}, \quad \forall k \neq l, \quad (2)$$

$$M_{S-T,k} = \mu\pi N_S N_T \frac{a_S^2 a_T^2 G_{S-T,k}}{4r_{S-T,k}^3} J_{S-T,k}, \quad (3)$$

<sup>1</sup>The phase of the signals transmitted by MI-WUSNs does not carry any relevant information as argued in [19].

<sup>2</sup>The phase of the transmitted signal is irrelevant, since only one sensor node transmits at a time.

<sup>3</sup>The factor 2 in the denominator is due to the calculation of the effective value of the sinusoidal voltage  $u_{in,S,k}(t)$ .

where  $\mu$  is the magnetic permeability, and  $r_{S-S,k,l}$  and  $r_{S-T,k}$  denote the distance between sensor  $k$  and other sensor  $l$  or between sensor  $k$  and the target node, respectively. Furthermore,  $G_{S-S,k,l}$  and  $G_{S-T,k}$  represent an additional attenuation due to the conductive medium (soil) for the respective signal transmissions. We assume that all nodes are placed in homogeneous medium, such that  $G_{\{\cdot\}} = e^{-r_{\{\cdot\}}\sqrt{\pi f_0 \mu \sigma}}$  holds with a constant soil conductivity  $\sigma$ . In addition, we assume that all coils' axes are orthogonal to the ground surface, such that the polarization factors  $J_{S-S,k,l}$  and  $J_{S-T,k}$  for the respective  $S-S$  and  $S-T$  cases are equal to 1, cf. [5]. Of course, in practice, the orientation of the wearable target node can be random. However, the influence of the coil orientation on the localization accuracy is beyond the scope of this work, since it requires a more extensive and deeper analysis.

Obviously,  $M_{S-S,k,l} = M_{S-S,l,k}$  holds, such that we define  $Z_{S-S,k,l} = Z_{S-S,l,k} = j2\pi f_0 M_{S-S,k,l}$  and  $Z_{S-T,k} = j2\pi f_0 M_{S-T,k}$  using (2)-(3). In addition, the inner impedance of the sensor and target node circuits at the resonance frequency  $f_0$  is given by  $Z_{in,S} = R_S + R_{L,S} = 2R_S$  and  $Z_{in,T} = R_T + R_{L,T} = 2R_T$ , respectively. For convenience, we stack all input voltages of the sensor nodes in a vector  $\mathbf{u}_S = [\hat{u}_{in,S,1}, \dots, \hat{u}_{in,S,N_{sn}}]^T$ . Similarly, the current vector  $\mathbf{i}_S$  contains the complex-valued current amplitudes of the sensor node circuits. Since we assume that the target node does not transmit any signal,  $\hat{u}_{in,T} = 0$  holds. In addition,  $i_T$  denotes the complex-valued amplitude of the current in the target node. In order to calculate the currents in all circuits, a set of voltage equations

$$\begin{bmatrix} \mathbf{u}_S \\ 0 \end{bmatrix} = \mathbf{Z}_{\text{total}} \cdot \begin{bmatrix} \mathbf{i}_S \\ i_T \end{bmatrix} = \begin{bmatrix} \mathbf{Z}_{S-S} & \mathbf{Z}_{S-T} \\ \mathbf{Z}_{S-T}^T & Z_{in,T} \end{bmatrix} \cdot \begin{bmatrix} \mathbf{i}_S \\ i_T \end{bmatrix} \quad (4)$$

needs to be solved, where the impedance matrices in (4) are given by

$$\mathbf{Z}_{S-S} = \begin{bmatrix} Z_{in,S} & Z_{S-S,1,2} & \cdots & Z_{S-S,1,N_{sn}} \\ Z_{S-S,1,2} & Z_{in,S} & \cdots & Z_{S-S,2,N_{sn}} \\ \vdots & \vdots & \ddots & \vdots \\ Z_{S-S,1,N_{sn}} & Z_{S-S,2,N_{sn}} & \cdots & Z_{in,S} \end{bmatrix}, \quad (5)$$

$$\mathbf{Z}_{S-T} = [Z_{S-T,1} \quad Z_{S-T,2} \quad \cdots \quad Z_{S-T,N_{sn}}]^T. \quad (6)$$

The solution of this set of equations is found by calculating the inverse of  $\mathbf{Z}_{\text{total}}$ . Hence, we obtain

$$\mathbf{i}_S = \mathbf{Z}_{S-S}^{-1} \mathbf{u}_S + \mathbf{A} \mathbf{u}_S, \quad (7)$$

cf. [21], with

$$\mathbf{A} = \mathbf{Z}_{S-S}^{-1} \mathbf{Z}_{S-T} (Z_{in,T} - \mathbf{Z}_{S-T}^T \mathbf{Z}_{S-S}^{-1} \mathbf{Z}_{S-T})^{-1} \mathbf{Z}_{S-T}^T \mathbf{Z}_{S-S}^{-1}. \quad (8)$$

The received signal at node  $l$  corresponds to the voltage  $\hat{u}_{out,S,l} = i_{S,l} R_{L,S} = \mathbf{e}_l^T \mathbf{Z}_{S-S}^{-1} \mathbf{u}_S R_{L,S} + \mathbf{e}_l^T \mathbf{A} \mathbf{u}_S R_{L,S}$ , where  $\mathbf{e}_l = [0, \dots, 0, 1, 0, \dots, 0]^T$  with the '1' at the  $l$ th position.

Obviously, the first component  $\hat{u}_{out,S,l,\text{known}} = \mathbf{e}_l^T \mathbf{Z}_{S-S}^{-1} \mathbf{u}_S R_{L,S}$  of  $\hat{u}_{out,S,l}$  only depends on the stationary deployed sensor nodes and can be assumed to be perfectly known to the processing

unit<sup>4</sup>. Hence, it can be easily subtracted from the received signal, similarly to [19]. The remaining part  $\Delta \hat{u}_{out,S,l} = \hat{u}_{out,S,l} - \hat{u}_{out,S,l,\text{known}} = \mathbf{e}_l^T \mathbf{A} \mathbf{u}_S R_{L,S}$  corresponds to the influence of the target node on the signal transmission and on the received signals at the sensor nodes. For the localization, the data collection is done in multiple time slots, where only one sensor node is allowed to transmit per time slot<sup>5</sup>. Hence, the voltage vector  $\mathbf{u}_S$  in time slot  $l$  can be expressed as  $\mathbf{u}_S = \mathbf{e}_l \hat{u}_{in,S,1}$ .

Due to large transmission distances between any two sensor nodes in the network (typically distances between 20 m and 40 m), we can assume weak couplings between them, such that we can use the approximation  $\mathbf{Z}_{S-S} \approx \mathbf{I} \cdot 2R_S$  with the identity matrix  $\mathbf{I}$ . Hence,  $\mathbf{A}$  can be simplified as

$$\mathbf{A} \approx \frac{\mathbf{Z}_{S-T} \mathbf{Z}_{S-T}^T}{(2R_S)^2 \left( Z_{in,T} - \frac{\mathbf{Z}_{S-T}^T \mathbf{Z}_{S-T}}{2R_S} \right)}. \quad (9)$$

With the definition of  $\mathbf{Z}_{S-T}$  from (6), we obtain  $\mathbf{Z}_{S-T}^T \mathbf{Z}_{S-T} = \sum_{n=1}^{N_{sn}} Z_{S-T,n}^2$  and

$$\begin{aligned} \Delta \hat{u}_{out,S,l} &\approx \frac{\mathbf{e}_l^T \mathbf{Z}_{S-T} \mathbf{Z}_{S-T}^T \mathbf{e}_l \hat{u}_{in,S,1}}{2 \left( 4R_S R_T - \sum_{n=1}^{N_{sn}} Z_{S-T,n}^2 \right)} \\ &= \frac{Z_{S-T,l}^2 \hat{u}_{in,S,1}}{2 \left( 4R_S R_T - \sum_{n=1}^{N_{sn}} Z_{S-T,n}^2 \right)}. \end{aligned} \quad (10)$$

Via summation of  $\Delta \hat{u}_{out,S,l}$  and reformulation, we arrive at

$$\sum_{n=1}^{N_{sn}} Z_{S-T,n}^2 \approx \frac{8R_S R_T \sum_{l=1}^{N_{sn}} \Delta \hat{u}_{out,S,l}}{\hat{u}_{in,S,1} + 2 \sum_{l=1}^{N_{sn}} \Delta \hat{u}_{out,S,l}}. \quad (11)$$

The substitution of (11) in (10) leads to

$$Z_{S-T,l}^2 \approx \frac{8R_S R_T \Delta \hat{u}_{out,S,l}}{\hat{u}_{in,S,1} + 2 \sum_{n=1}^{N_{sn}} \Delta \hat{u}_{out,S,n}}, \quad (12)$$

from which the mutual inductance  $M_{S-T,l}$  and correspondingly the distance between sensor  $l$  and the target node can be deduced using (3).

Due to the network deployment in a dense medium with a substantial electrical conductivity, the influence of the signals from other communication systems on the signal detection in MI-WUSNs can be neglected. Hence, we focus on the thermal noise as the main source of disturbance, which is generated in the resistors  $R_S$  and  $R_{L,S}$  of the sensor nodes' circuits and represented by additional voltage sources  $u_{\text{noise},in,l}(t)$ ,  $\forall l$ . Using the results from [22] and [5], the variance of the noise

<sup>4</sup>In practice, the coupling between sensor nodes can vary as well. Hence,  $\hat{u}_{out,S,l,\text{known}}$  may deviate from its assumed value. However, this deviation would only become significant, if the distance between sensor node  $l$  and any other sensor node is shorter than the distance between node  $l$  and the target node. Since the sensor nodes are typically deployed in substantial distance from each other for a better coverage, this situation may only occur at the sensor nodes far away from the target node. The respective receive signals are very weak and therefore not used for localization.

<sup>5</sup>Multiple simultaneous transmissions would cause mutual interference and dramatically reduce the localization performance.

$u_{\text{noise,out},l}(t)$ ,  $\forall l$  received at the respective load impedance can be given by

$$\text{Var}\{u_{\text{noise,out},l}(t)\} \approx 4KT (R_S + R_{L,S}) \frac{R_{L,S}^2}{(R_S + R_{L,S})^2}, \quad (13)$$

where  $K$  stands for the Boltzmann constant and  $T = 290$  K ( $\triangleq 17^\circ$  C) is the assumed temperature in Kelvin. As observed in [19], this low-power noise can still significantly degrade the system performance, if the useful signal is acquired at the load resistor of the transmitter. Hence, in order to improve the reliability of the signal detection,  $\Delta \hat{u}_{\text{out},S,l}$ ,  $\forall l$  is sampled and averaged within each time slot, such that a reasonable level of noise suppression is achieved. In our simulations, we assume a noise suppression of 30 dB corresponding to an averaging over 1000 samples.

### III. LOCALIZATION IN MI-WUSNS

In the following, we study two localization techniques. The first technique is the well-known trilateration, which is used in the traditional positioning systems. Unfortunately, a closely related method, triangulation, based on the angular diversity of the received signal cannot be employed in MI-WUSNs, since only one coil with an omnidirectional transmission pattern<sup>6</sup> is employed per sensor node. Therefore, we utilize a machine learning based localization technique as our second method, which might provide sufficient localization accuracy if the trilateration fails.

#### A. Trilateration

Due to its simplicity and robustness, trilateration is employed in almost all existing positioning systems. This approach utilizes the measurements of the signal strength acquired at different locations and deduces the distances from these locations to the target to be localized based on the measurements.

In order to obtain a unique localization solution in a three-dimensional space, four signals are required. However, additional information, for instance that the target node is supposed to be located on the earth surface, is usually available. This information allows for a reduction of the complexity of the problem and an exclusion of some of the erroneous solutions. Hence, three signals are typically sufficient in order to determine a small region of possible locations in a three-dimensional space. In our work, we consider a two-dimensional space and three signals would yield a unique solution. Unfortunately, no additional information is available that would prioritize the selection of certain locations. Hence, we utilize three signals from the three sensor nodes  $k$ ,  $l$ , and  $m$ , which receive the strongest signals among all sensor

nodes<sup>7</sup>. The distances from these nodes to the target node are denoted as  $r_{S-T,k}$ ,  $r_{S-T,l}$ , and  $r_{S-T,m}$ , respectively. Hence, the following set of quadratic equations needs to be solved:

$$\begin{aligned} (x_T - x_{S,k})^2 + (y_T - y_{S,k})^2 &= r_{S-T,k}^2, \\ (x_T - x_{S,l})^2 + (y_T - y_{S,l})^2 &= r_{S-T,l}^2, \\ (x_T - x_{S,m})^2 + (y_T - y_{S,m})^2 &= r_{S-T,m}^2, \end{aligned} \quad (14)$$

where  $(x_T, y_T)$ ,  $(x_{S,k}, y_{S,k})$ ,  $(x_{S,l}, y_{S,l})$ , and  $(x_{S,m}, y_{S,m})$  are the  $x$ - and  $y$ -coordinates of the target node and the three sensor nodes  $k$ ,  $l$ , and  $m$ , respectively.

In MI-WUSNs, the use of trilateration may not always be accurate due to the non-linearity of the channel model with respect to the distance between any two coils. In order to show this, we deduce the mutual inductance from (12):

$$M_{S-T,l}^2 \approx -\frac{8R_S R_T \Delta \hat{u}_{\text{out},S,l}}{\left(\hat{u}_{\text{in},S,1} + 2 \sum_{n=1}^{N_{sn}} \Delta \hat{u}_{\text{out},S,n}\right) 4\pi^2 f_0^2}. \quad (15)$$

The substitution of (3) into (15) yields

$$e^{r_{S-T,l} \sqrt{\pi f_0 \mu \sigma}} r_{S-T,l}^3 = \alpha \quad (16)$$

with  $\alpha \approx \sqrt{\frac{(f_0 \mu \pi^2 N_S N_T a_S^2 a_T^2)^2 (\hat{u}_{\text{in},S,1} + 2 \sum_{n=1}^{N_{sn}} \Delta \hat{u}_{\text{out},S,n})}{32 R_S R_T \Delta \hat{u}_{\text{out},S,l}}}$ .

Unfortunately, no closed-form solution for this type of equations is known. Instead, a numerical calculation using the so-called Lambert-W function can be applied, cf. [23]. In this context, the additive noise can dramatically reduce the localization performance, since even a small error in the signal magnitude can lead to a dramatically wrong distance estimation.

#### B. Machine Learning based Localization

The main principle of machine learning based localization in WSNs has been described in [18] and [24], according to which the whole plane is split into possible positions or areas, which represent different classes. If the target node is located in one of these areas, the received signal at the sensor nodes may have some properties, that are typical for such a situation. Hence, it might be possible to distinguish between the areas based on the received signal and to determine the most likely area, at which the target node is located. For this, a machine learning algorithm can be used. Due to the stationary deployment of the MI-WUSNs, the supervised learning is preferable over other types of machine learning (e.g. unsupervised learning), since the training of the classifier can be done offline and the relevant properties of the received signals can be accurately learned. In particular, the use of Support Vector Machines (SVMs) seems promising. An SVM is a classifier that determines the optimal separating hyperplane between two classes of vectors, such that the closest distance between any vector from both classes and the hyperplane is maximized. Hence, the

<sup>7</sup>Theoretically, more than three signals can be used for trilateration (the so-called multilateration approach). However, due to much weaker signals received at the respective additional sensor nodes, the accuracy improvement does not justify the complexity increase. In many cases, even a worse localization accuracy can be observed, which is due to the impact of the received noise signals.

<sup>6</sup>Since we assume that all coils' axes show to the ground surface, an omnidirectional signal propagation from/to each coil results.

diversity of the available signal properties (so-called features) is fully exploited. In [24], the localization in WSNs using SVMs with multiple classes has been described. For this, an iterative method has been proposed. In each iteration, the field with possible positions is split into two classes, left and right half fields, respectively. Using an SVM, the most likely half field is selected and then analyzed in the same way in the next iteration. The procedure repeats itself for a given number of iterations, which corresponds to the granularity of the localization. Then, the middle of the finally retained field is selected as the most likely position of the target. The benefit of this strategy lies in the reduced complexity, since more and more positions are excluded from the analysis with each iteration. For example, after the first iteration, the focus of the classification is on the selected (e.g. right) half field, which means that the other (left) half field is not considered anymore. Unfortunately, this strategy is very vulnerable to the classification errors in each iteration, since wrong decisions lead to a selection of the wrong half field, which can cause a substantial deviation of the estimated position from the true one.

### C. Proposed Method

In this work, we make use of SVM based localization similar to [24]. However, in order to increase the accuracy, the so-called "One-Against-One" classification with multiple classes is applied, cf. [25]. In this approach, the whole field of possible positions is split into multiple areas. Each area (e.g. area  $q$ ) is compared with all other areas using the respective SVMs and the received signal. Moreover, each area is assigned a weight  $\varrho_q = 0, \forall q$ , initially. If the classifier chooses area  $q$  over area  $s$ , its weight increases by one, i.e.,  $\varrho_q \leftarrow \varrho_q + 1$ . Obviously, the area with the largest final weight corresponds to the most likely position of the target node, since the features of the received signal fit best to this area. Hence, this strategy provides on average a better accuracy than the approach in [24]. However, the number of pairs of areas to test increases with the squared number of dedicated areas, which may become a crucial factor for the system complexity and computational effort.

In order to reduce the system complexity while preserving the localization accuracy, we consider multiple subfields and apply the mentioned "One-Against-One" localization method to each subfield separately. Hereafter, the most promising subfield is determined and the respective estimated position is selected. For this, a square subfield of a moderate size around each sensor node is considered. This subfield is then split into  $N_{\text{areas}}$  areas, which may correspond to a potential target location. In each area, a set of  $N_{\text{train}}$  positions is selected, with which the training data is obtained. An example of the total arrangement of the subfields, areas and training positions is shown in Fig. 2. Since the areas in different subfields are not compared with each other directly, the complexity of the proposed method is substantially reduced compared to the original "One-Against-One" localization technique.

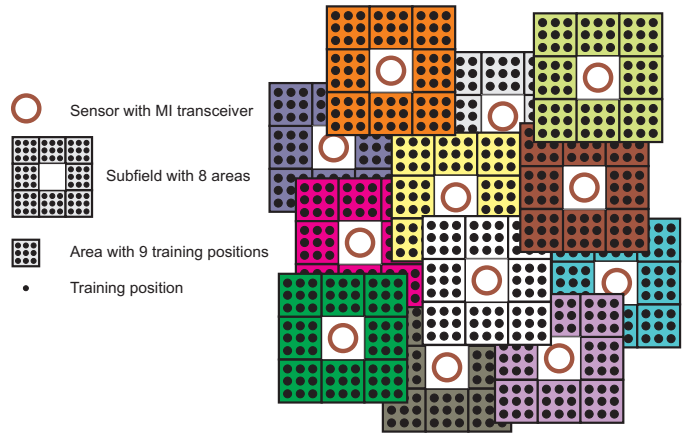


Fig. 2. Example of MI-WUSN with overlapping subfields divided into 8 areas each for the training of SVMs. From each area, 9 training positions are selected.

1) *Training mode:* In each subfield,  $N_{\text{areas}} \cdot (N_{\text{areas}} - 1)$  SVMs need to be trained. The training of the SVMs is done offline, as mentioned earlier. For this, the target node is assumed to be in one of the  $N_{\text{train}}$  dedicated positions of one area, which implies that the couplings between all coils are calculated for this scenario. Correspondingly, the received signals  $\Delta \hat{u}_{\text{out},s,l}, \forall l$ , are determined according to Section II. These signals are processed in order to extract the most relevant features. The choice of relevant features and its representation is a non-trivial task, which is usually handled by an experienced system designer for each particular application. Unfortunately, no optimal method of feature extraction for MI-WUSNs is known to date. Hence, we propose our own strategy below.

2) *Feature extraction:* According to the previous discussion, there are multiple issues that need to be taken into account for the feature selection. Typically, the importance of the feature increases with increasing signal strength. Correspondingly, the features carried by a weak signal (low signal strength) might be suppressed since they do not have enough weight for the classification. In order to take into account as many features as possible, the magnitude of all  $N_{sn}$  received signals is replaced by its logarithmic representation. Basically, the logarithmic scale ensures that multiple signals with different orders of magnitude can be fairly compared. In addition, signal elements that are lower than a certain threshold  $\tau$  are clipped to 0. This yields an additional noise suppression, since the low-power fluctuations of the weak and noisy signals are mitigated. The value of  $\tau$  is set to 50 dB below the maximal signal strength among all received signals. The resulting set of the clipped logarithmically scaled signal magnitudes is stacked in a vector (called feature vector) and used for training and classification.

3) *Prediction mode:* After all SVMs in all subfields are trained, the classification of the actual received feature vector (called prediction) can be performed. This procedure is usually called prediction. Using the received feature vector, each SVM

decides between the respective two areas. This binary decision is then used in the mentioned "One-Against-One" algorithm in each subfield. Hence, the most likely area of each subfield is determined and the respective middle points of the selected areas indicate the most likely position of the target node in the considered subfield. This yields a total set of  $N_{sn}$  predicted positions. In order to select the most likely position from this set, we assume the presence of the target node in all  $N_{sn}$  positions of the set and calculate the respective feature vectors. Using these vectors a position of the target is selected, which yields the lowest squared error with respect to the true feature vector based on the actual received signal.

#### D. Hybrid Localization

The accuracy of the proposed localization based on SVMs is governed by many parameters. In some situations, despite a noise suppression of 30 dB, the noise might corrupt the features of the received signals so much, that the machine learning based localization becomes infeasible. On the other hand, there might be situations where the trilateration is very accurate. Therefore, we investigate a hybrid scheme, where both methods (trilateration and SVMs) are combined and the overall most likely position of the target is determined. For this, we first execute both methods and obtain the estimated target positions with them. Then, the respective feature vectors based on the estimated positions are determined similarly to the prediction mode. These vectors are compared with the true received feature vector and the method resulting in the smallest deviation is selected. The corresponding position of the target node is the final estimate of the target location.

### IV. NUMERICAL RESULTS

In our simulations, we consider sensor networks with randomly distributed sensor nodes deployed in a square field of  $100 \text{ m} \times 100 \text{ m}$  size. We assume a common resonance frequency<sup>8</sup>  $f_0 = 1 \text{ MHz}$  and equal transmit power  $P_k = P = 10 \text{ mW}$  in each sensor node  $k$ . For the sensor coils, we assume  $N_S = 1000$  turns and a radius  $a_S = 25 \text{ cm}$ . For the target node, we assume  $N_S = 100$  turns and a radius  $a_T = 5 \text{ cm}$ . The wire radius is set to  $0.5 \text{ mm}$  for all coils. The conductivity of soil is set to  $\sigma = 0.01 \text{ S/m}$  according to [7]. All SVMs are trained using a Gaussian kernel with optimized scaling via cross-validated SVMs. The size of the subfields to be investigated in the neighborhood of each sensor node is  $25 \text{ m} \times 25 \text{ m}$ . Each subfield is split into  $N_{\text{areas}} = 49$  areas with identical size. The number of training vectors is  $N_{\text{train}} = 25$  for each area. In each simulation, we consider 100 different networks and 20 possible positions of the target for each network. For each position, we perform the localization using the discussed methods and calculate the resulting localization error. In the following, the performance is shown in terms of the cumulative distribution function (CDF) of the localization error.

<sup>8</sup>In general, this choice of the resonance frequency does not maximize the localization accuracy or the network throughput [5]. However, the optimization of the system parameters for these criteria is beyond the scope of this work.

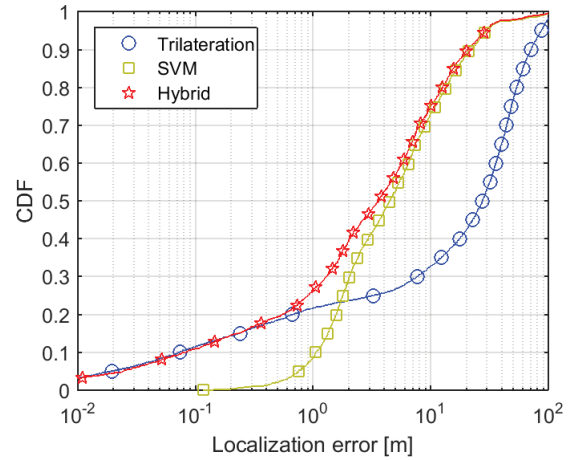


Fig. 3. Cumulative distribution of the localization error with  $N_{sn} = 15$  sensor nodes.

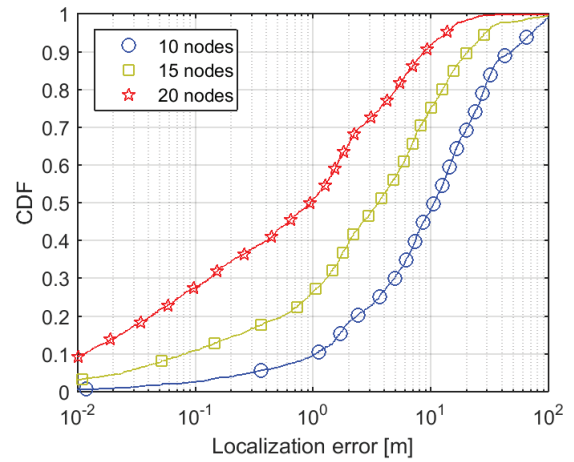


Fig. 4. Cumulative distribution of the localization error using hybrid method and different numbers of nodes.

At first, we discuss results for the localization using  $N_{sn} = 15$  sensor nodes according to Fig. 3. We observe a huge possible localization error of up to 100 m for all considered schemes. For the SVM based localization (and correspondingly for the hybrid method), large errors result from the possible selection of wrong subfields due to the noise influence. However, this performance degradation has occurred only in 5% of the considered cases. The SVM based localization outperforms the trilateration in up to 71% of the cases (as observed using additional simulations) and obviously reduces the maximum localization error significantly. The hybrid method combines the benefits of both methods and therefore its CDF converges to the CDF of the trilateration for small localization errors and to the CDF of the SVMs for large localization errors.

Due to the obvious advantage of the hybrid scheme, we show its performance for different numbers of sensor nodes in Fig. 4. We observe a substantial decrease of the localization error with increasing number of sensor nodes. This is expected, since more features can be utilized for classification. Also, the average distance between the target node and the nearest

sensor node in the network reduces. Hence, both methods, i.e., trilateration and SVM based localization, perform better and the hybrid scheme can localize 50% of targets with an error  $\leq 1$  m for 20 nodes,  $\leq 3.6$  m for 15 nodes, and  $\leq 10.5$  m for 10 nodes, respectively. Moreover, 20% of the targets can be localized with an error of  $\leq 4$  cm for 20 nodes,  $\leq 55$  cm for 15 nodes, and  $\leq 2.3$  m for 10 nodes, respectively. In order to further improve the performance of localization in MI-WUSNs, either larger coils have to be employed or the transmit power has to be increased. However, these system parameters are bounded by the constraints of system design and need to be carefully optimized. This optimization remains for future investigations.

## V. CONCLUSION

In this work, a novel passive localization technique for MI-WUSNs has been presented, which enables the localization of a silent target node without any explicit signaling from this node. The presence of the target node is detected by exploiting the coupling between all magnetic devices and extracting the relevant information from the received signals at the respective sensor nodes. Here, the distances between sensor nodes and the target node cannot always be precisely deduced from the extracted received signals due to a complicated path loss function, which includes polynomials and exponentials. Correspondingly, the traditional localization approach based on trilateration becomes inaccurate and a machine learning algorithm employing Support Vector Machines has been presented. For a further improvement of the localization accuracy, this approach has been combined with the trilateration by selecting the more precise result based on the relative receive signal error, such that a hybrid method results. This hybrid method shows a good performance in terms of localization accuracy in most of the investigated cases. In addition, by increasing the number of sensor nodes, the localization accuracy can be substantially improved.

## REFERENCES

- [1] I.F. Akyildiz and E.P. Stuntebeck, "Wireless underground sensor networks: Research challenges," *Ad Hoc Networks*, vol. 4, no. 6, pp. 669–686, Nov. 2006.
- [2] M.C. Vuran and A.R. Silva, "Communication Through Soil in Wireless Underground Sensor Network: Theory and Practice," in *Sensor Networks*, G. Ferrari, Ed. Springer Berlin Heidelberg, 2009.
- [3] Z. Sun and I.F. Akyildiz, "Magnetic induction communications for wireless underground sensor networks," *IEEE Trans. Antennas Propag.*, vol. 58, no. 7, pp. 2426–2435, Jul. 2010.
- [4] —, "On capacity of magnetic induction-based wireless underground sensor networks," in *Proc. of IEEE INFOCOM 2012*, Mar. 2012, pp. 370–378.
- [5] S. Kisseleff, I.F. Akyildiz, and W.H. Gerstacker, "Throughput of the Magnetic Induction Based Wireless Underground Sensor Networks: Key Optimization Techniques," *IEEE Trans. on Communications*, vol. 62, no. 12, pp. 4426–4439, December 2014.
- [6] S.-C. Lin, I.F. Akyildiz, P. Wang, and Z. Sun, "Distributed Cross-Layer Protocol Design for Magnetic Induction Communication in Wireless Underground Sensor Networks," *IEEE Trans. on Communications*, vol. 14, no. 7, pp. 4006–4019, July 2015.
- [7] A. Markham and N. Trigoni, "Magneto-inductive networked rescue system (MINERS) taking sensor networks underground," in *Proc. of IPSN 2012*, April 2012.
- [8] X. Tan, Z. Sun, and I.F. Akyildiz, "A Testbed of Magnetic Induction-based Communication System for Underground Applications," *arXiv:1503.02519*, March 2015.
- [9] J. Ma, X. Zhang, Q. Huang, and L. Cheng, "Experimental Study on the Impact of Soil Conductivity on Underground Magneto-Inductive Channel," *IEEE Antennas and Wireless Propagation Letters*, April 2015.
- [10] K. Mori, "Application of Weight Functions to the Magnetic Localization of an Object," *IEEE Transactions on Magnetics*, vol. 25, no. 3, pp. 2726–2731, May 1989.
- [11] X. Tan and Z. Sun, "Environment-Aware Indoor Localization using Magnetic Induction," in *Proc. of the IEEE GlobeCom*, December 2015.
- [12] E.A. Prigge and J.P. How, "Signal architecture for a distributed magnetic local positioning system," *IEEE Sensors Journal*, vol. 4, no. 6, pp. 864–873, December 2004.
- [13] A. Markham, N. Trigoni, S.A. Ellwood, and D.W. Macdonald, "Revealing the hidden lives of underground animals using magneto-inductive tracking," in *Proc. of the 8th ACM Conference on Embedded Networked Sensor Systems (SenSys)*, November 2010.
- [14] A. Markham, N. Trigoni, D.W. Macdonald, and S.A. Ellwood, "Underground Localization in 3-D Using Magneto-Inductive Tracking," *IEEE Sensors Journal*, vol. 12, no. 6, pp. 1809–1816, June 2012.
- [15] X. Huang, W. Zhu, and D. Lu, "Underground miners localization system based on ZigBee and WebGIS," in *Proc. of the 18th International Conference on Geoinformatics*, June 2010.
- [16] S.R. Rusu, M.J.D. Hayes, and J.A. Marshall, "Localization in large-scale underground environments with RFID," in *Proc. of the 24th Canadian Conference on Electrical and Computer Engineering (CCECE)*, May 2011.
- [17] S. Kisseleff, I.F. Akyildiz, and W. Gerstacker, "Disaster detection in magnetic induction based wireless sensor networks with limited feedback," in *Proc. of IFIP Wireless Days*, November 2014.
- [18] G. Mao and B. Fidan, *Localization Algorithms and Strategies for Wireless Sensor Networks*. IGI Global, 2009.
- [19] S. Kisseleff, I.F. Akyildiz, and W. Gerstacker, "Transmitter-Side Channel Estimation in Magnetic Induction based Communication Systems," in *Proc. of IEEE BlackSeaCom 2014*, May 2014.
- [20] A. Karalis, J.D. Joannopoulos, and M. Soljacic, "Efficient wireless non-radiative mid-range energy transfer," *Annals of Physics*, vol. 323, no. 1, pp. 34–48, Jan. 2008.
- [21] D. Bernstein, *Matrix Mathematics*. Princeton University Press, 2005.
- [22] R.R.A. Syms and L. Solymar, "Noise in metamaterials," *J. Appl. Phys.*, vol. 109, no. 124909, June 2011.
- [23] D.A. Barry, J.-Y. Parlange, L.Li, H. Prommer, C.J. Cunningham, F. Stagnitti, "Analytical approximations for real values of the Lambert W - function," *Mathematics and Computers in Simulation (Elsevier)*, vol. 53, no. 1, pp. 95–103, August 2000.
- [24] D.A. Tran and T. Nguyen, "Localization in Wireless Sensor Networks Based on Support Vector Machines," *IEEE Transactions on Parallel and Distributed Systems*, vol. 19, no. 7, pp. 981–994, July 2006.
- [25] C.-W. Hsu and C.-J. Lin, "A comparison of methods for multiclass support vector machines," *IEEE Transactions on Neural Networks*, vol. 13, no. 2, pp. 415–425, March 2002.